Original Article

Asian Pacific Journal of Tropical Biomedicine

journal homepage: www.apjtb.org

doi: 10.4103/2221-1691.300729

Impact Factor: 1.90

Network pharmacology-based analysis of effective components and mechanism of *Rhizoma coptidis* in treating diabetes

Qian-Qian Zeng[1#], Jia-Wei Cai[1#], Yue Xu[1], Lin Li[2], Qiu Chen[1✉], Ren-Song Yue[1✉]

[1]*Hospital of Chengdu University of Traditional Chinese Medicine, Chengdu 610072, P.R. China*

[2]*School of Pharmacy, Chengdu University of Traditional Chinese Medicine, Chengdu, 611130, PR China*

ABSTRACT

Objective: To identify the active ingredients, potential targets, and mechanism of *Rhizoma coptidis* by bioinformatics method, and to explore the hypoglycemic effect of *Rhizoma coptidis* by *in vitro* experiments.

Methods: The chemical components of *Rhizoma coptidis* were collected through database search, and oral bioavailability and drug-likeness were used for preliminary screening. The targets of *Rhizoma coptidis* and diabetes-related targets were collected by database retrieval and reverse docking techniques, and the biological process of cross-set proteins was analyzed. The inhibitory effects of *Rhizoma coptidis* on α-glucosidase, α-amylase activity, and advanced glycation end products (AGEs) were determined *via in vitro* experiments. In addition, the effects of *Rhizoma coptidis* on pre-adipocyte differentiation, absorption of glucose by adipocytes, and the level of intracellular triglyceride were investigated using the adipocyte differentiation model.

Results: There were 11 potentially active ingredients in *Rhizoma coptidis*. IL-6, caspase-3, epidermal growth factor receptor (*EGFR*), *MYC*, and estrogen receptor 1 were considered as the key genes. The bioinformatics analysis showed that *Rhizoma coptidis* played an anti-diabetic role mainly *via* biological processes and signaling pathways including hormone receptor activity, glutathione binding, steroid binding, *etc*. *In vitro* experiments showed that the extract of *Rhizoma coptidis* inhibited the activities of α-glucosidase and α-amylase, and the generation of AGEs; meanwhile, the extract promoted the absorption of glucose by adipocytes. In addition, the extract of *Rhizoma coptidis* decreased triglyceride level.

Conclusions: Our network pharmacology and *in vitro* experiments demonstrate the anti-diabetic effects and possible underlying mechanisms of *Rhizoma coptidis* extract.

KEYWORDS: *Rhizoma coptidis*; Diabetes; Network pharmacology; Target; Traditional Chinese medicine

1. Introduction

In the traditional Chinese medicine (TCM) theory, diabetes is classified as "Wasting-thirst", which is a comprehensive syndrome and mainly characterized by excessive drinking, excessive urination, excessive eating, emaciation, fatigue, and sweet urine; while in modern medicine, diabetes is considered as a common metabolic disease with complex pathogenesis, mainly characterized by chronic hyperglycemia. Currently, it is believed that the occurrence of diabetes is related to a variety of factors, such as defective insulin secretion, impaired biological action of insulin, and inflammatory response. The metabolism of diabetic patients could be affected, causing a series of metabolic disorders such as sugar, protein, fat, water, and electrolyte. In addition, long-term hyperglycemia could lead to chronic damage

✉To whom correspondence may be addressed. E-mail: chenqiu1005@cdutcm.edu.cn (Qiu Chen), songrenyue@cdutcm.edu.cn (Ren-Song Yue).
#: contributed equally to this paper.

How to cite this article: Zeng QQ, Cai JW, Xu Y, Li L, Chen Q, Yue RS. Network pharmacology-based analysis of effective components and mechanism of *Rhizoma coptidis* in treating diabetes. Asian Pac J Trop Biomed 2021; 11(1): 29-39.

Article history: Received 13 February 2020; Revision 12 April 2020; Accepted 25 June 2020; Available online 26 November 2020

and dysfunction of various tissues, especially eyes, kidney, heart, blood vessels, and nerves, then result in serious complications, such as diabetic nephropathy, diabetic retinopathy, and diabetic peripheral neuropathy and could seriously threaten the life and health of patients[1-3].

Rhizoma coptidis (*R. coptidis*) is an important traditional Chinese herbal medicine and has been widely used in the treatment of diabetes for thousands of years. It has remarkable curative effects with few side effects and low treatment cost[4,5]. At the same time, modern pharmacological studies have also found that extract of *R. coptidis* and its active components can inhibit the activity of glucosidase and disglucidases, interfere with the conversion of carbohydrates into monosaccharides and their absorption in the small intestine, and play an anti-diabetic role[6,7]. A study found that berberine, the alkaloid component of *R. coptidis*, can significantly inhibit the activity of disaccharidases in the protein kinase in a dependent pathway and reduce the mRNA expression of sucrase isomaltase complex in diabetic rats and normal rats[8]. These studies have proved that *R. coptidis* can directly control the rise of postprandial blood glucose levels by inhibiting carbohydrate digestion. In this study, network pharmacology was used to clarify the pharmacodynamic basis and mechanism of *R. coptidis* in the treatment of diabetes, and to provide references for the subsequent drug development of *R. coptidis*.

2. Materials and methods

2.1. Reagent

Phosphate buffer (PBS, 0.1 mol/L, pH 6.8), dimethyl sulfoxide (DMSO), methanol, starch, glucose and sodium carbonate (Na_2CO_3) were purchased from Chengdu Klong Chemical Reagent Factory; 3,5 dinitrosalicylic acidchromogen solutions (DNS) was purchased from Chengdu Riefensi Biotechnology Co.; α-glucosidase, α-amylase, bovine serum albumin (BSA), metformin and 4-nitrophenyl-beta-*D*-glucopyranoside (PNPG) were purchased from Sigma Company. Dulbecco's modified Eagle medium, fetal bovine serum, penicillin-streptomycin, and trypsin-ethylene diamine tetraacetic acid were purchased from Gibco Company. 3-(4,5-dimethyl-2-thiazolyl)-2,5-diphenyl-2-H-tetrazolium bromide (MTT) detection kit was purchased from Boster Biological Technology Company. 2-Deoxy-2-[(7-nitro-2,1,3 benzoxadiazol-4-yl) amino]-*D*-glucose (2-NBDG) was provided by Invitrogen Company. Triglyceride (TG) detection kit was purchased from Nanjing Jiancheng Biological Engineering Research Institute. 3T3-L1 pre-adipocytes were acquired from the Beina Biological Company.

2.2. Small molecule database establishment

The chemical components of *R. coptidis* were collected by searching the database of systematic pharmacology of traditional Chinese medicine, integrated pharmacology-based research platform of TCM V2.0 (www.tcmip.cn/TCMIP/index.), and integrated database of traditional Chinese medicine. Oral bioavailability (OB) and drug-likeness (DL) were used to screen the active compounds. Compounds with sufficient DL$\geqslant$0.18 and OB$\geqslant$30% were selected as candidate active ingredients. The 2D or 3D structures of the candidate compounds in PubChem (https://pubchem.ncbi.nlm.nih.gov/) and ChemSpider (http://www.chemspider.com/) were downloaded and saved as a MOL file format.

2.3. Target library establishment

The MOL files of candidate compounds were uploaded to pharmMapper (http://lilab.ecust.edu.cn/pharmmapper/index.php) online database and the potential targets of candidate compounds were identified by high-throughput screening. These target proteins were combined and the repeated collections of small molecule compounds were deleted. The Online Mendelian Inheritance in Man (https://omim.org/), DisGeNET (http:// www.disgenet.org/), TTD (http://bidd.nus.edu.sg/group/cjttd/), and other databases were searched with "diabetes" as the keyword, and the collection of targets of diseases was constructed by eliminating repeated targets. Finally, the small-molecule target set was combined with the disease target set, and the intersection was taken as the target protein library in this study. The standard names of all protein targets were determined by UniProt (http://www.uniprot.org/).

2.4. Bioinformatic annotation

Functional annotation and pathway enrichment analysis of proteins in the target library, including Gene Ontology (GO) and Kyoto Encyclopedia of Genes and Genomes (KEGG) pathway enrichment analysis, were carried out by R language software (3.6.3), and bar charts and bubble charts were drawn. Only the top 20 functions or pathways with the most significant enrichment were shown in the pictures. $P<0.05$ was considered statistically significant. Finally, the potential molecular mechanism of the anti-diabetic effect of *R. coptidis* was comprehensively analyzed.

2.5. Protein-protein interaction (PPI) network construction

Proteins from the previously obtained target library were uploaded to the string online database to predict PPI and the study species was restricted to human sources. The analysis results were downloaded and saved in TSV format and imported into Cytoscape software (3.6.0) to construct the PPI network of *R. coptidis*-targets-diabetes. The CytohHubba plug-in and R language (3.6.3) software were used to analyze the hub genes in PPI.

2.6. Network construction

The R language tool was used to construct the compound-target protein data pair and the data pair was imported into Cytoscape software to construct the drug-molecular-target-disease network diagram (DMTD). In this network diagram, the nodes represent drugs, compounds, target proteins, and diseases; while the edges represent the interrelationships between the nodes. Finally, the importance of each node in the network was evaluated by calculating the three topological feature data: degree, average shortest path length, betweenness centrality, and closeness centrality.

2.7. In vitro studies

2.7.1. Preparation of lyophilized powder of R. coptidis extract (RCE)

R. coptidis was purchased from Neautus Chinese Herbal Pieces Ltd. Co., and identified by Prof. Ren-Song Yue of Chengdu University of TCM (HL20191205). A total of 200 g *R. coptidis* was added to distilled water at a ratio of 1:10, decocted twice for 1 h every time. The liquid was collected and filtered with gauze and the filtrate was centrifuged (12000 *g*, 10 min). The supernatant was taken and freeze dried at a low temperature to obtain the lyophilized powder of *R. coptidis*.

2.7.2. Experiment on inhibition of α-glucosidase activity

The inhibitory effect of RCE on the activity of α-glucosidase was determined based on the method of Pierre *et al*. with some modifications[9]. Briefly, the RCE was first dissolved in PBS containing 10% DMSO and then diluted to different concentrations (0.75-24 mg/mL) for later use. A certain amount of PBS, 20 μL PNPG (0.5 mmol/L), and 20 μL RCE with different concentrations were added to the 96-well plate in turn, and the mixture system was 100 μL. The mixture was oscillated in a water bath at 37 ℃ for 10 min, added with 10 μL of α-glucosidase (0.2 U/mL), mixed well and reacted in a water bath at 37 ℃ for 20 min. Finally, 150 μL Na_2CO_3 solution (0.2 mol/L) was added to stop the reaction and the absorbance (OD) of each hole was measured at 405 nm immediately with a microplate. In this study, drugs and α-glucosidase were not added to the blank group, and the RCE was replaced by equal volume PBS as the negative control. Meanwhile, the blank control was set to exclude the influence of drug color on the experimental results (no α-glucosidase solution was added). Each experiment was repeated three times. According to the following formula, the inhibition rate of α-glucosidase activity was calculated.

Inhibition rate (%) = $[1-(OD_{RCE}-OD_{blank\ of\ drug})/(OD_{negative\ control}-OD_{blank})]\times 100\%$

2.7.3. Experiment on inhibition of α-amylase activity

A total of 0.5 mL of α-amylase (0.686 mg/mL) was added into the test tube, then 0.5 mL of RCE with different concentrations was added, mixed evenly, and placed in a water bath at 37 ℃ for 5 min. A total of 0.5 mL 1% soluble starch solution was added, mixed, and reacted for 5 min. Then 0.5 mL DNS was added immediately to color and stop the reaction. The mixture was boiled in boiling water for 5 min, then cooled down to room temperature for 20 min. The volume was set to 5 mL with PBS and the OD of the solution was measured at 540 nm wavelength with a UV-visible spectrophotometer (UV-2550, Shimadzu, Japan). In this study, 0.5 mL PBS was used as the blank control, and the RCE was replaced by equal volume PBS as the negative control. As the experiment of α-glucosidase, the blank control was set to exclude the influence of drug color on the experimental results (no addition of α-amylase). Each experiment was repeated three times. The inhibition rate (%) of the samples with different concentrations to the alpha-amylase was calculated according to the following formula:

Inhibition rate (%) = $[1-(OD_{RCE}-OD_{blank\ of\ drug})/(OD_{negative\ control}-OD_{blank})]\times 100\%$

2.7.4. Inhibition experiment of advanced glycation end products (AGEs) generation

Fluorescence spectrophotometry (RF-6000, Shimadzu, Japan) was used to detect the inhibitory effect of RCE on AGEs generation. Extract of RCE at different concentrations was added to 1 mL sterile bovine serum albumin (30 mg/mL) and 1 mL glucose solution (0.5 mol/L), mixed evenly, then sealed and incubated for 14 d at 37 ℃ in darkness. Fluorescence absorption (FA) of AGEs (emission wavelength 420 nm, excitation wavelength 350 nm) was determined by fluorescence spectrophotometry at room temperature. In this experiment, no drugs or glucose were added to the blank group and the RCE was replaced by PBS of equal volume as the negative control. As mentioned above, the blank control was set to exclude the influence of drug fluorescence absorption on the experimental results (no glucose was added). Each experiment was repeated three times. According to the following formula, the inhibition rate of samples with different concentrations on AGEs generation was calculated.

Inhibition rate (%) = $[1-(FA_{RCE}-FA_{blank\ of\ drug})/(FA_{negative\ control}-FA_{blank})]\times 100\%$

2.7.5. Cell viability detection

The 3T3-L1 pre-adipocytes were inoculated into 96-well plates (1×10^4/well) and cultured in an incubator for 24 h. After 24 h, the new medium was replaced. In addition to the normal group, cells in other groups were added with different concentrations of RCE (0-3.2 mg/mL) and incubated for 48 h. After 48 h, the MTT method

was used to determine the effect of RCE on the activity of 3T3-L1 pre-adipocytes. In short, 20 μL MTT was added to each well and incubated for another 4 h. The medium was sucked out carefully in the well. A total of 150 μL DMSO solution was added to the well and then the 96-well plate was placed on a low-speed shaking table to oscillate for 10 min until the microcrystals were completely dissolved. The absorbance value of each well was measured at 490 nm using an enzyme marker and the viability of each group of cells was calculated.

Cell viability %= ($OD_{experimental\ group}$ /$OD_{normal\ group}$)×100%

2.7.6. Effects of RCE on adipocyte differentiation

The "cocktail method" is often used to cause the 3T3-L1 pre-adipocytes to differentiate into mature adipocytes, which can well simulate the process of adipocyte differentiation *in vitro*. In this study, this method was used to induce cell differentiation, and oil red O was used for specific staining of fat. A single-cell suspension was prepared from 3T3-L1 pre-adipocytes in the logarithmic growth stage, seeded in a 96-well culture plate (1×10^4/well), and cultured for 24 h in a constant temperature incubator at 37 ℃ and 5% CO_2. When the confluence of cells reached more than 90%, the treatment to promote differentiation was carried out. In addition to the normal group, the cells in the other groups were cultured in the lipid induction medium [complete medium containing 1 μmol/L dexamethasone, 0.5 mmol/L 3-Isobutyl-1-methylxanthine (IBMX), 10 μg/mL insulin, and 200 μmol/L indomethacin] for 2 d, followed by complete medium containing 10 μg/mL insulin for 2 d, then by complete medium (without insulin) for 10 d. At the same time of inducing differentiation, cells in the drug group were treated with different concentrations of RCE (0.1, 0.2, 0.4 mg/mL), and cells in the positive group were treated with metformin (100 μmol/L)[10]. After induction, the cells were fixed with 10% formalin for 10 min, treated with 60% isopropanol for 5 min, completely dried at room temperature, and stained with oil red dye for 30 min. Finally, isopropanol was added to the 96-well plate to dissolve the oil red dye. After the oil red in the fat cells was fully dissolved, an enzyme marker was used to detect the OD value of each group at 510 nm.

2.7.7. Glucose uptake assay

With reference to the method described by Alonso-Castro *et al*.[11], the effect of RCE on glucose uptake by fat cells was evaluated by 2-deoxyglucose uptake assay. The well-differentiated 3T3-L1 pre-adipocytes were inoculated into 96-well plates (1×10^4/well) and placed in an incubator for further culture for 24 h. After the cells were completely adherent to the wall, the cells in the other groups were added with different concentrations of RCE (0.1, 0.2, 0.4 mg/mL) or metformin (100 μmol/L) for 48 h. After treatment, 100 μmol/L 2-NBDG was added to each well for incubation for 30 min. Subsequently, the absorption of 2-NBDG was determined at 485 nm/535 nm with a fluorescein marker. The experiments were repeated three times, and the data were expressed by the average of the results of the three experiments.

2.7.8. Detection of intracellular TG

Differentiated 3T3-L1 pre-adipocytes were inoculated into a 6-well plate (1×10^6/well) and cultured in an incubator for 24 h. After the cells were completely adherent to the wall, RCE was treated with different concentrations (0.1, 0.2, 0.4 mg/mL) for 48 h, and cells in the positive group were treated with metformin (100 μmol/L). After the treatment, the cells were collected and broken by ultrasound. The TG content in cells was detected according to the manufacturer's instructions of the TG detection kit. The experiments were repeated three times and the data were expressed by the average of the results of the three experiments.

2.8. Statistical analysis

All the data in this study were analyzed by SPSS 19.0 software. The results were expressed as mean±SD and the differences between groups were analyzed by one-way ANOVA. $P<0.05$ indicated that the difference was statistically significant.

3. Results

3.1. Active anti-diabetic compound of R. coptidis

According to database search and literature mining, 352 compounds in *R. coptidis* were collected. Then, screening was conducted according to the screening criteria of DL≥0.18 and OB≥30%, and finally, 14 small molecule compounds with efficacy were obtained. The information of the compounds is shown in Table 1.

3.2. Diabetic targets of active compounds

Through high-throughput screening, 90 targets of *R. coptidis* were obtained. A total of 10221 diabetes targets were collected through database search and literature review. By comparing drug targets with disease targets, 84 overlapping targets were obtained.

3.3. GO analysis of target genes

The GO functions of these target genes were enriched and analyzed by R language software, and the analysis results showed that the diabetic protein genes of active components of *R. coptidis* were mainly enriched in 81 biological processes. It mainly involved

Table 1. Information on compounds in *Rhizoma coptidis*.

ID	Mol ID	Molecule name	Molecular weight	AlogP	OB(%)	DL
C1	MOL002668	Worenine	334.37	3.73	45.83	0.87
C2	MOL000098	Quercetin	302.25	1.50	46.43	0.28
C3	MOL000622	Magnograndiolide	266.37	1.18	63.71	0.19
C4	MOL002897	Epiberberine	336.39	3.45	43.09	0.78
C5	MOL002907	Corchoroside A	404.55	1.34	104.95	0.78
C6	MOL001458	Coptisine	320.34	3.25	30.67	0.86
C7	MOL002904	Berlambine	351.38	2.49	36.68	0.82
C8	MOL002894	Berberrubine	322.36	3.20	35.74	0.73
C9	MOL001454	Berberine	336.39	3.45	36.86	0.78
C10	MOL002903	(R)-canadine	339.42	3.40	55.37	0.77
C11	MOL000785	Palmatine	352.44	3.65	64.60	0.65
C12	MOL013352	Obacunone	454.56	2.68	43.29	0.77
C13	MOL000762	Palmidin A	510.52	4.52	35.36	0.65
C14	MOL008647	Moupinamide	313.38	2.86	86.71	0.26

OB: bioavailability; DL: drug-likeness.

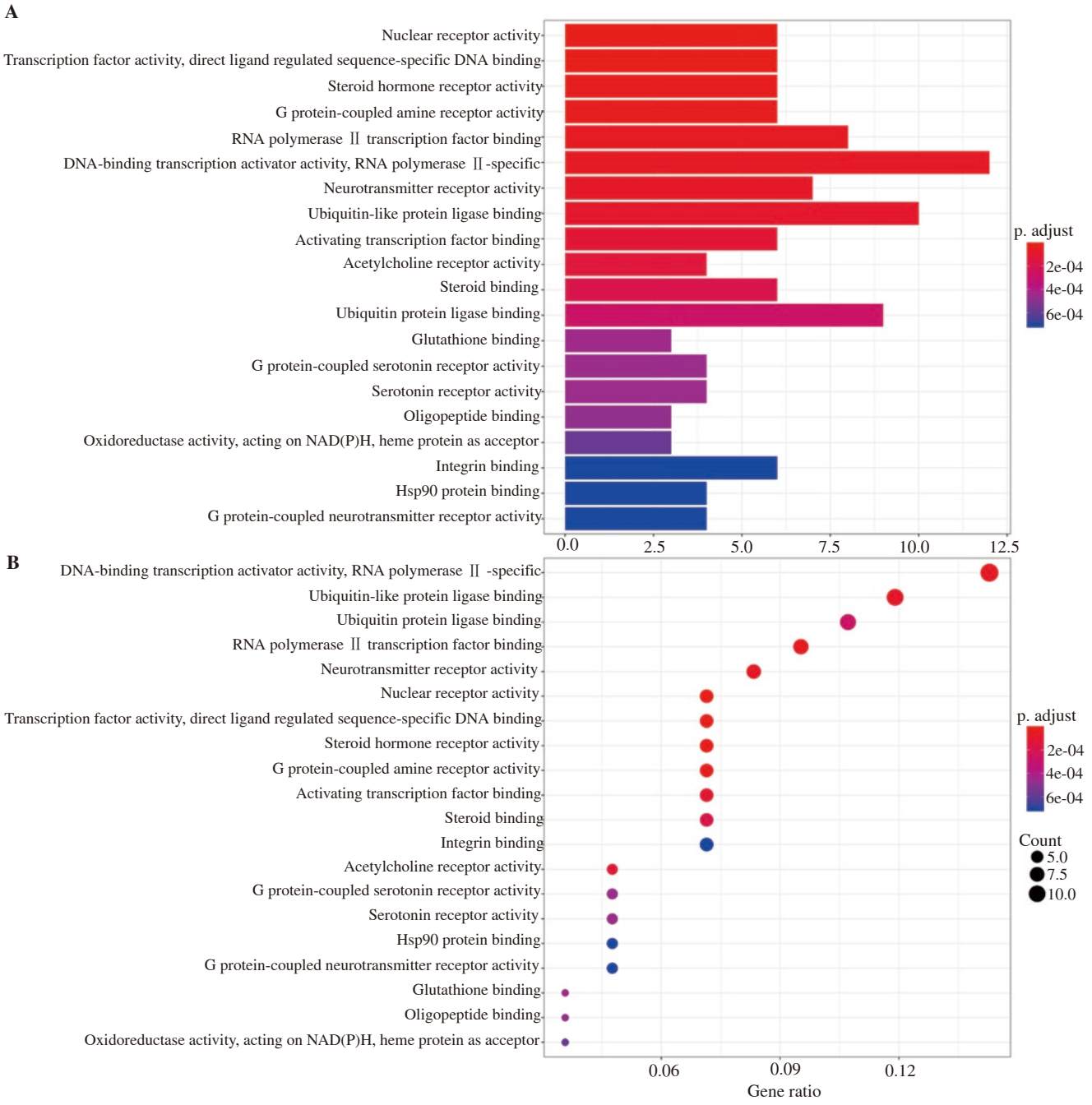

Figure 1. Gene Ontology (GO) functions enrichment of overlapping target genes (Top 20). A: Bar chart of GO; B: Bubble chart of GO.

hormone receptor activity, G protein-coupled amine receptor activity, ubiquitin-like protein ligase binding, acetylcholine receptor activity, steroid binding, glutathione binding, G protein-coupled serotonin receptor activity, *etc*. It indicates that *R. coptidis* can play an anti-diabetic role by participating in a variety of biological processes (Figure 1 & Supplementary Table 1).

3.4. KEGG pathway enrichment analysis

The KEGG pathways of these target genes were enriched and analyzed by R language software, and a total of 80 significant pathways were obtained (P<0.05). As shown in Figure 2 and Supplementary Table 2, the main pathways included AGE-RAGE signaling pathway in diabetic complications, proteoglycans in

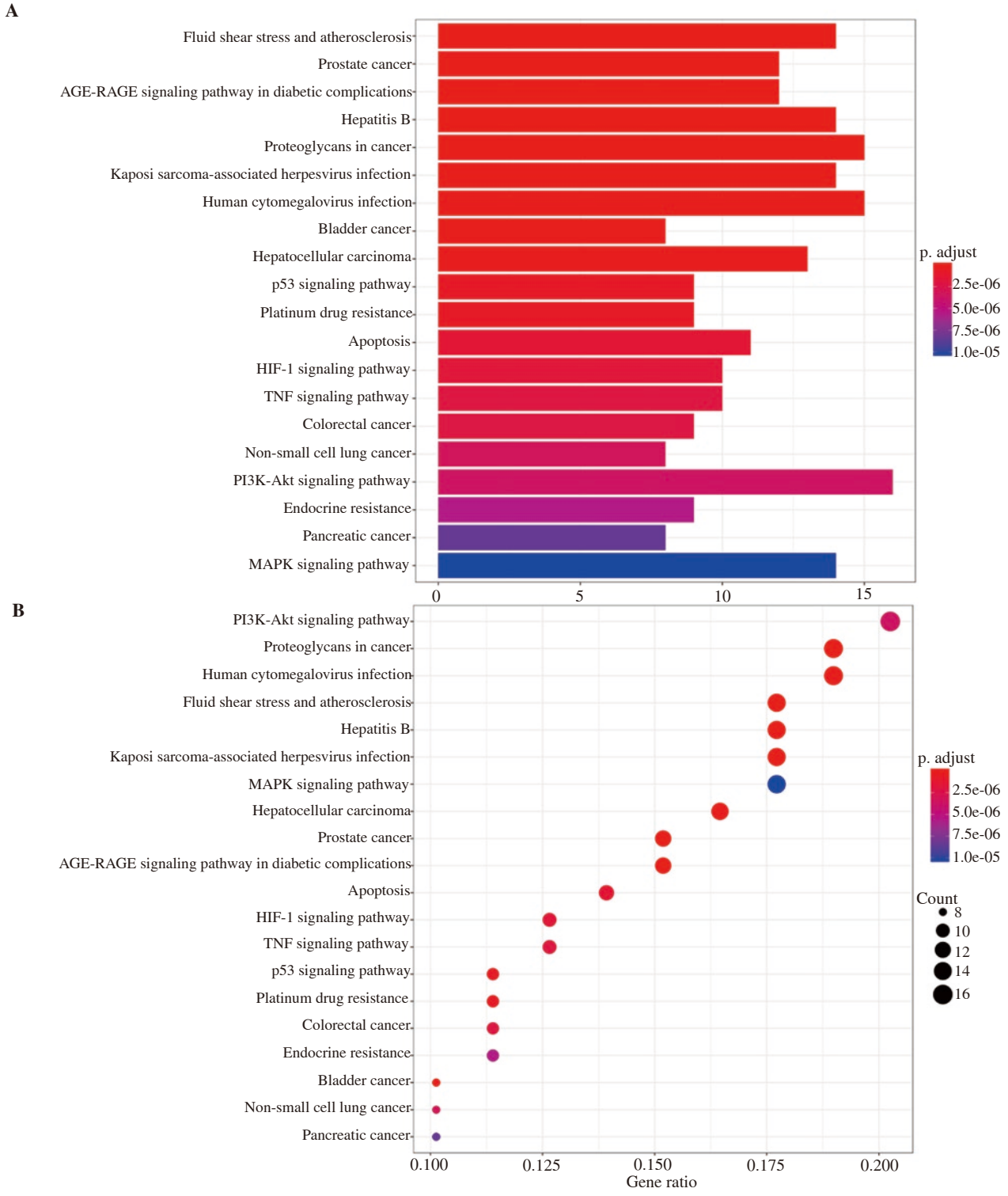

Figure 2. Kyoto Encyclopedia of Genes and Genomes (KEGG) pathways analysis of overlapping target genes (top 20). A: Bar chart of KEGG; B: Bubble chart of KEGG.

cancer, hypoxia-inducible factor-1 signaling pathway, tumor necrosis factor (TNF) signaling pathway, PI3K-Akt signaling pathway, endocrine resistance, and a variety of cancer-related pathways (such as prostate cancer, bladder cancer, liver cancer, colorectal cancer, non-small cell lung cancer, *etc*).

3.5. PPI analysis

In PPI, the nodes represent proteins and the connections between nodes represent the interactions between two proteins. The analysis revealed that IL-6, caspase-3, epidermal growth factor receptor, vascular endothelial growth factor A, MYC, estrogen receptor 1, *etc*. were key targets of *R. coptidis* for the treatment of diabetes (Figure 3A&B).

3.6. DMTD

After sorting and analyzing the previously retrieved data through R software, a total of 122 pairs of molecular-target data were obtained and imported into Cytoscape software to obtain DMTD. The results are shown in Figure 4. In this network diagram, there were 94 nodes and 122 edges, including 11 compounds (the targets of the three compounds were not included in the overlapping targets) and 84 targets. The circle represents the target, the square represents the component, and the hexagon represents the drug and disease. The network parameter information of all active compounds is shown in Table 2.

Tabe 2. Network parameter information of all active compounds.

Name	Degree	Average shortest path length	Betweenness centrality	Closeness centrality
C1	5	2.781	0.002	0.360
C2	73	1.385	0.352	0.722
C3	3	2.823	0.001	0.354
C4	6	2.760	0.001	0.362
C5	3	2.823	0.001	0.354
C6	5	2.781	0.001	0.360
C7	7	2.740	0.003	0.365
C8	6	2.760	0.001	0.362
C9	7	2.740	0.002	0.365
C10	10	2.677	0.010	0.374
C11	8	2.719	0.004	0.368

3.7. Anti-diabetic effect of R. coptidis in vitro

As shown in Figure 5A, RCE of different concentrations had a significant inhibitory effect on the activity of α-glucosidase, with the inhibitory rate of high concentration of RCE over 80%. Similarly, RCE showed the same significant inhibitory effect on the activity of α-amylase and the inhibitory effect was dose-dependent (Figure 5B). In addition, 0.75 mg/mL-24 mg/mL RCE significantly inhibited the generation of AGEs *in vitro* (Figure 5C).

3.8. Cell viability assay

As shown in Figure 6A, RCE of lower than 0.8 mg/mL had little effect on the viability of 3T3-L1 pre-adipocytes. However, as the concentration of RCE gradually increased, the influence on the viability of cells increased, indicating that the low concentration

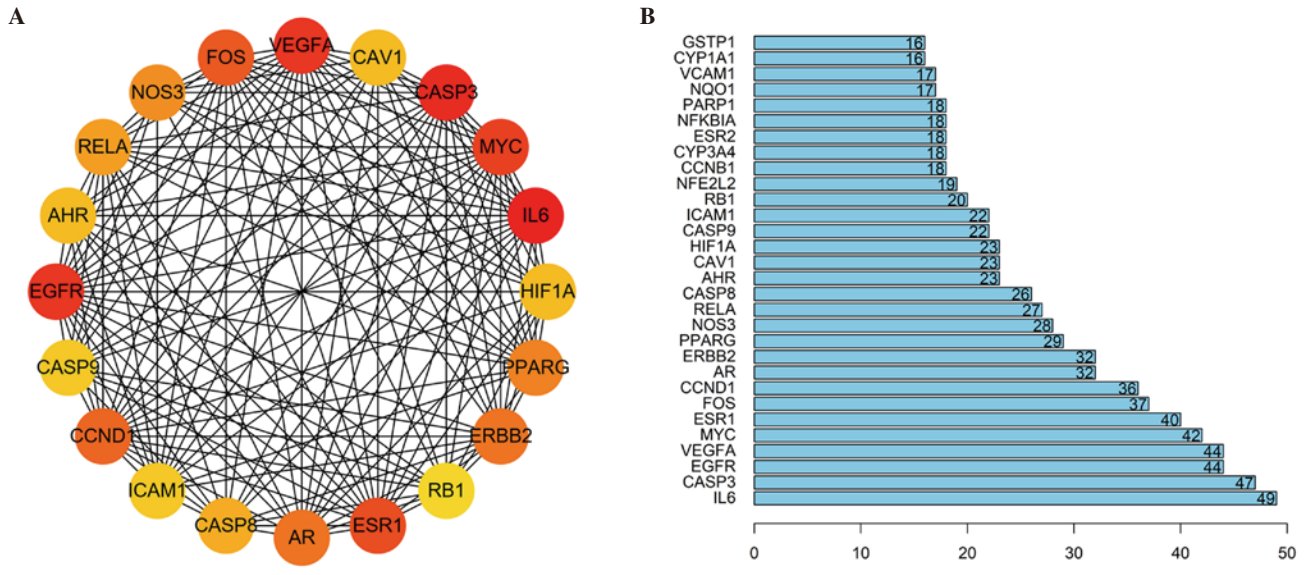

Figure 3. Protein-protein interaction network (PPI) of overlapping target genes. A: The key genes of *Rhizoma coptidis* in PPI (Cytoscape); B: The key genes of *Rhizoma coptidis* in PPI (R software).

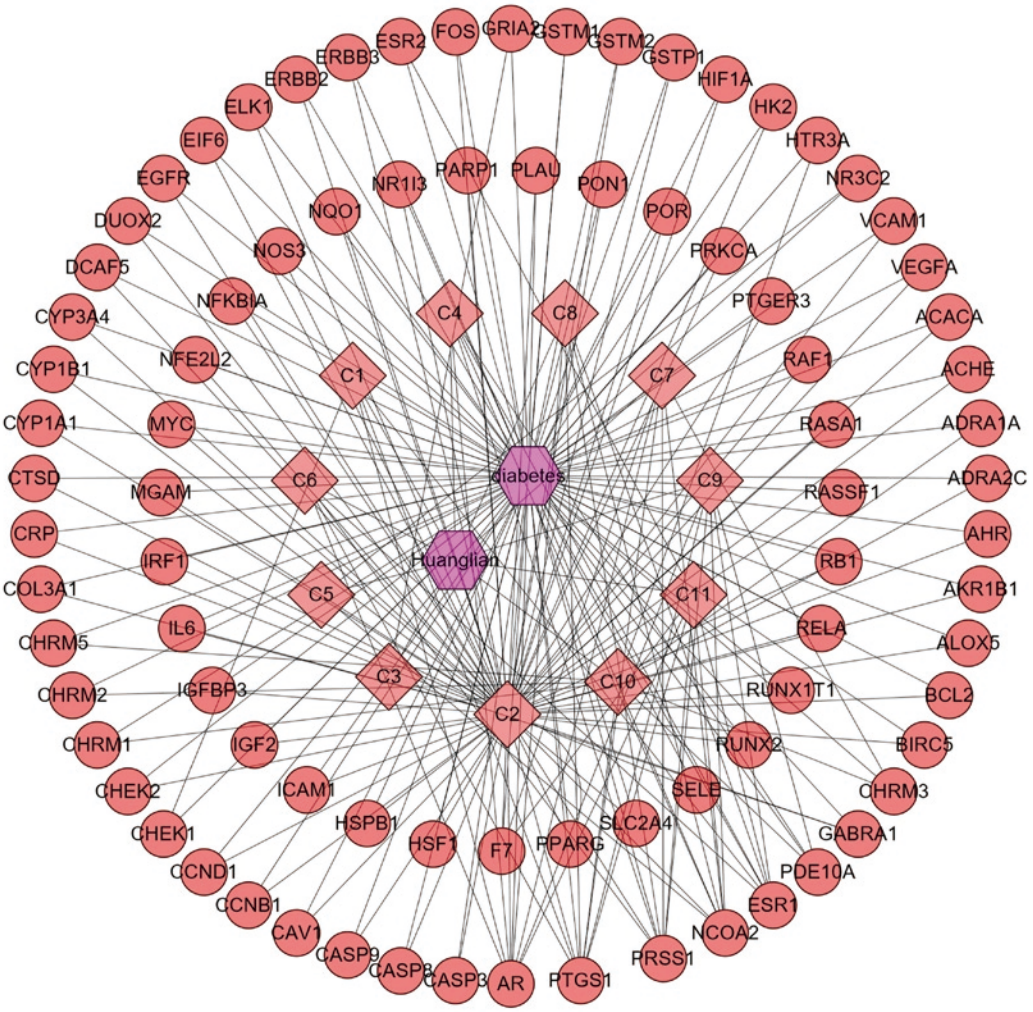

Figure 4. Drug-molecular-target-disease network diagram. The circle represents the target, the square represents the component, and the hexagon represents the drug and disease.

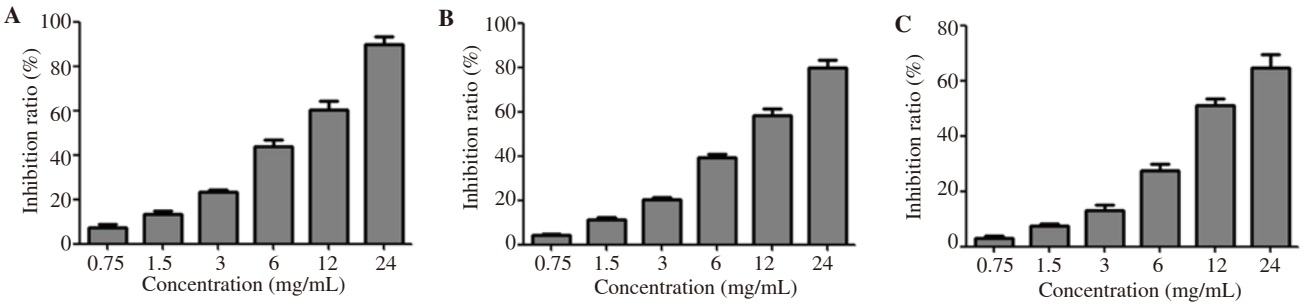

Figure 5. Anti-diabetic effect of *Rhizoma coptidis in vitro*. A: Experiment on the inhibition of α-glucosidase activity; B: Experiment on the inhibition of α-amylase activity; C: Inhibition experiment of advanced glycation end products generation.

of RCE had no toxic effect on cells. Therefore, in the following experiments, we adopted RCE dosing of 0.1 mg/mL, 0.2 mg/mL and 0.4 mg/mL.

3.9. RCE inhibits adipocyte differentiation

As shown in Figure 6B, compared with the normal group, the OD value of the cells in the control group was significantly increased. It indicated that a large number of lipid droplets were present in the cytoplasm and the pre-adipocytes were successfully induced to differentiate into adipocytes. The results showed that different concentrations of RCE had significant inhibition on adipocyte differentiation, and this inhibition was dose-dependent. Interestingly, the positive drug metformin seemed to have little effect on adipocyte differentiation.

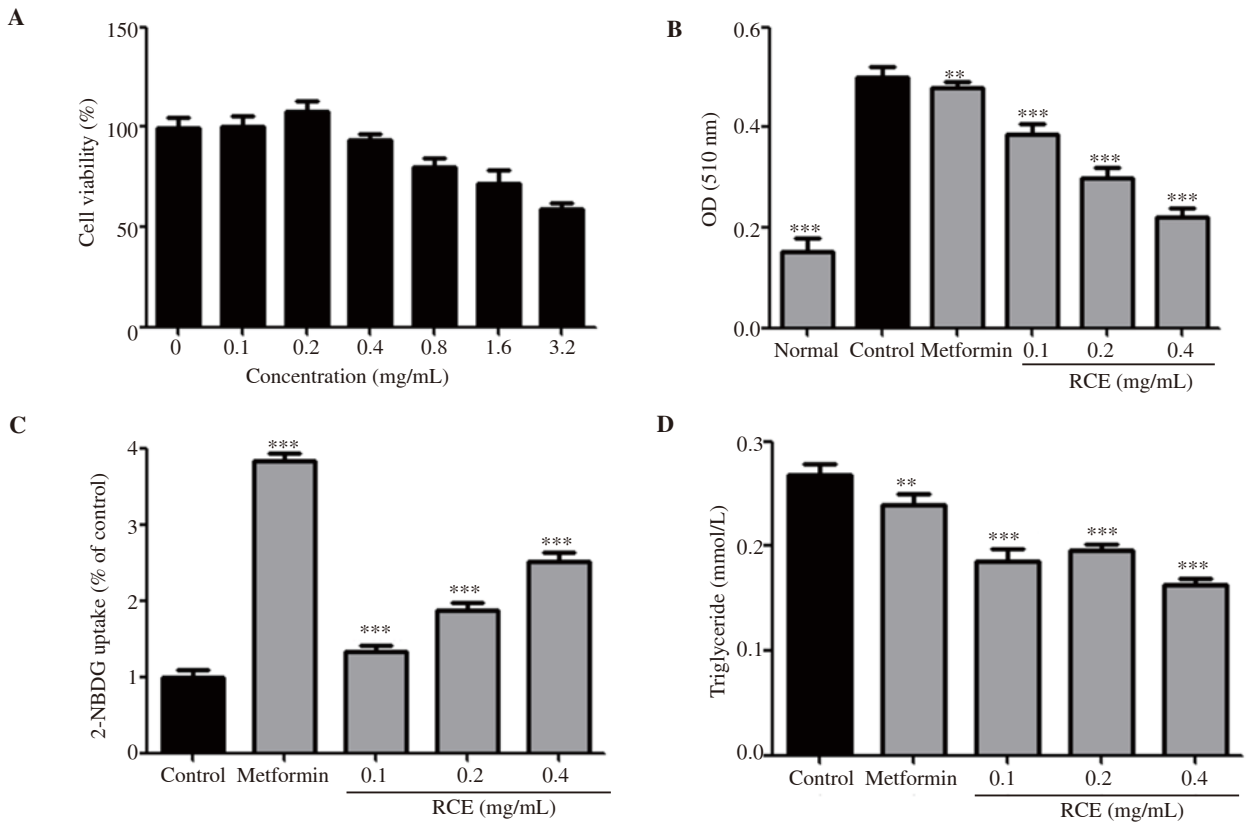

Figure 6. Intervention of extract of *Rhizoma coptidis* (RCE) on 3T3-L1 pre-adipocytes. A: Cell viability assay; B: effect of RCE on adipocyte differentiation; C: effect of RCE on glucose uptake in cells; D: effect of RCE on lipid metabolism in adipocytes. $^{**}P<0.05$, $^{***}P<0.01$, compared with control.

3.10. RCE promotes glucose uptake by adipocytes

In this study, we investigated the effect of RCE on 2-deoxyglucose uptake by adipocytes. As shown in Figure 6C, the metformin intervention significantly increased glucose uptake in fat cells compared to the control cells. Similarly, RCE also showed a promoting effect in a dose dependent manner. These results suggest that RCE effectively increases glucose uptake in differentiated adipocytes.

3.11. RCE improves lipid metabolism in adipocytes

As shown in Figure 6D, compared with mature fat cells, both metformin and RCE reduced the TG level in cells and the reduction effect of RCE was more significant. It is suggested that RCE can reduce the content of TG in fat cells to improve the disorder of lipid metabolism.

4. Discussion

Diabetes is an incurable metabolic disease characterized by insulin resistance and inadequate insulin secretion[12,13]. At present, the common clinical treatment for diabetes includes insulin injection and oral chemical hypoglycemic agents. However, these treatments have obvious adverse reactions, such as hypoglycemia and gastrointestinal reactions[14]. Herbal medicines have received a lot of attention because of their high efficacy and low side effects in the treatment of diseases[15,16].

TCM believes that the human body is an organic whole, with each tissue and organ communicating with each other structurally, coordinating and serving each other functionally, and also influencing each other in pathology. Therefore, all drugs in TCM play their therapeutic role through multiple channels and targets, which are consistent with the systematic biology thought of network pharmacology. A growing number of studies have found that *R. coptidis*, an important natural drug, has an obvious anti-diabetes effect[17,18]. In this study, network pharmacology was applied to explore the anti-diabetes effect of *R. coptidis* and analyze the active ingredients and targets of *R. coptidis* for the treatment of diabetes. The results showed that 11 chemical components of *R. coptidis* were closely related to their anti-diabetic effects, including worenine, quercetin, magnograndiolide, epiberberine, corchoroside A, coptisine, berlambine, berberrubine, berberine, (R)-canadine, and palmatine. Through visual analysis, it was found that quercetin, (R)-canadine, and palmatine might be the main active ingredients of *R. coptidis* for the treatment of diabetes. Currently, studies have found that quercetin has a significant anti-diabetic effect. It can

reduce blood glucose by improving the antioxidant status of the pancreas of type 2 diabetic rats and regulating the enzyme activity related to glucose metabolism[19]. In addition, studies have found that quercetin can also improve learning and memory impairment in diabetic rats[20]. Similarly, palmatine therapy has been reported to alleviate neuropathic pain and depressive behavior in diabetes by inhibiting ERK1/2 phosphorylation and TNF-α and IL-1β release in the hippocampus[21]. PPI analysis of the targets of *R. coptidis* showed that IL-6 was one of the key targets for the action of *R. coptidis*. In addition, the key targets also include caspase-3, epidermal growth factor receptor, vascular endothelial growth factor A, MYC, estrogen receptor 1, and other targets. These targets have been shown to have an anti-inflammatory effect on diabetes, such as IL-6, which can improve glucose metabolism and play an important role in the treatment of diabetes[22-24]. The consistency of our results with those in previous studies proves the reliability of the results of network pharmacology.

Bioinformatics annotation of overlapping targets showed that these targets were mainly involved in biological processes such as hormone receptor activity, G protein-coupled amine receptor activity, ubiquitin-like protein ligase binding, acetylcholine receptor activity, steroid binding, ubiquitin-protein ligase binding, glutathione binding, G protein-coupled serotonin receptor activity, *etc*., and involved in pathways such as AGE-RAGE signaling pathway in diabetic complications, proteoglycans in cancer, hypoxia inducible factor-1 signaling pathway, TNF signaling pathway, PI3K-Akt signaling pathway, endocrine resistance, *etc*. Modern studies have demonstrated that these biological processes and pathways are involved in the development and progression of diabetes in multiple ways[25,26]. Our study indicates that *R. coptidis* can play an anti-diabetic role by participating in multiple biological processes *in vivo* through multi-component action and multiple targets.

α-Glucosidase plays an important role in the food absorption, food digestion in the intestinal mucosa, and decomposition of starch into glucose[27]. Inhibition of α-glucosidase activity slows the rate at which starch is broken down into glucose and glucose is absorbed in the small intestine. It is worth noting that this process does not generally increase insulin secretion and does not cause hypoglycemia. Therefore, inhibition of α-glucosidase activity is of great significance for the control of glucose homeostasis. α-Amylase can promote the hydrolysis and digestion of carbohydrates in the food. The inhibition of its activity can reduce body sugar absorption, reduce the content of blood glucose and lipid, reduce the synthesis of fat, and induce weight loss[28]. Studies have found that the serum and tissue levels of AGEs in diabetic patients are significantly higher than normal people, and more and more studies have shown that AGEs play an important role in the development of diabetes[29-31]. Natural drugs with the above three activities can be used as a supplement or substitute for diabetes management. The results of this study proved that *R. coptidis* had significant inhibitory effects on α-glucosidase, α-amylase, and AGEs generation *in vitro* and preliminarily verified the anti-diabetic effect of *R. coptidis*. To preliminarily explore the mechanism of action of *R. coptidis* to treat diabetes, we established the differentiation of the adipose cell model. The results showed that *R. coptidis* inhibited the differentiation of pre-adipocytes and promoted the glucose uptake of adipocytes. In addition, *R. coptidis* has a regulatory effect on lipid metabolism disorders in cells by decreasing TG level.

In this study, network pharmacology was used for the first time to explore the scientificity and reliability of *R. coptidis* in the treatment of diabetes from the perspective of multiple components and multiple targets, and it could provide new ideas for the systematic study of TCM.

Conflict of interest statement

We declare that there is no conflict of interest.

Funding

This work was supported by the Sichuan Special Project of TCM Science and Technology Research (No.2016C034).

Authors' contributions

QQZ, JWC, QC, and RSY contributed to the conception and design of the study, acquisition, analysis, and interpretation of data, drafting and revising the article and final approval of the version to be published. YX and LL contributed to the analysis of data, drafting the article and final approval of the version to be published.

References

[1] Konig M, Lamos EM, Stein SA, Davis SN. An insight into the recent diabetes trials: What is the best approach to prevent macrovascular and microvascular complications? *Curr Diabetes Rev* 2013; **9**(5): 371-381.

[2] Rios JL, Francini F, Schinella GR. Natural products for the treatment of type 2 diabetes mellitus. *Planta Med* 2015; **81**(12-13): 975-994.

[3] Labazi H, Trask AJ. Coronary microvascular disease as an early culprit in the pathophysiology of diabetes and metabolic syndrome. *Pharmacol Res* 2017; **123**: 114-121.

[4] Zhou JY, Zhou SW, Zhang KB, Tang JL, Guang LX, Ying Y, et al. Chronic effects of berberine on blood, liver glucolipid metabolism and liver PPARs expression in diabetic hyperlipidemic rats. *Biol Pharm Bull* 2008; **31**(6): 1169-1176.

[5] Wang H, Mu W, Shang H, Lin J, Lei X. The antihyperglycemic effects of *Rhizoma coptidis* and mechanism of actions: A review of systematic reviews and pharmacological research. *Biomed Res Int* 2014; **2014**: 798093.

[6] Chen L, Wang X, Liu Y, Di X. Dual-target screening of bioactive components from traditional Chinese medicines by hollow fiber-based ligand fishing combined with liquid chromatography-mass spectrometry. *J Pharm Biomed Anal* 2017; **143**: 269-276.

[7] Hui T, Lei C, Fang T, Yuan B, Lin Q. Rb2 inhibits α-glucosidase and regulates glucose metabolism by activating AMPK pathways in HepG2 cells. *J Funct Foods* 2017; **28**: 306-313.

[8] Liu L, Yu YL, Yang JS, Li Y, Liu YW, Liang Y, et al. Berberine suppresses intestinal disaccharidases with beneficial metabolic effects in diabetic states, evidences from *in vivo* and *in vitro* study. *Naunyn Schmiedebergs Arch Pharmacol* 2010; **381**(4): 371-381.

[9] Pierre C, Tremblay, Roland R, Dube JY. *p*-Nitrophenol-a-glucopyramoside as substrate for measurement of maltase activity in human semen. *Clin Chem* 1978; **24**: 208-211.

[10]Murad A, Abeer A, Reem AJ, Srinivasa B, Dwaipayan S, Janardhana B, et al. Anti-diabetic activities of *Dactylorhiza hatagirea* leaf extract in 3T3-L1 cell line model. *Pharmac Mag* 2019; **15**(64): 212-217.

[11]Alonso-Castro AJ, Miranda-Torres AC, Gonzalez-Chavez MM, Salazar-Olivo LA. *Cecropia obtusifolia* Bertol and its active compound, chlorogenic acid, stimulate 2NBD glucose uptake in both insulin-sensitive and insulin-resistant 3T3 adipocytes. *J Ethnopharmacol* 2008; **3**: 458-464.

[12]DeFronzo RA. Pathogenesis of type 2 diabetes mellitus. *Med Clin North Am* 2004; **88**(4): 787-835.

[13]Zhu Y, Zhang C. Prevalence of gestational diabetes and risk of progression to type 2 diabetes: A global perspective. *Curr Diab Rep* 2016; **16**(1): 7.

[14]Teng H, Chen L. α-Glucosidase and α-amylase inhibitors from seed oil: A review of liposoluble substance to treat diabetes. *Crit Rev Food Sci Nutr* 2017; **57**(16): 3438-3448.

[15]Zhang Q, Liu J, Zhang MM, Wei SJ, Li RL, Gao YX, et al. Apoptosis induction of fibroblast-like synoviocytes is an important molecular-mechanism for herbal medicine along with its active components in treating rheumatoid arthritis. *Biomolecules* 2019; **9**: 795.

[16]Peng W, Shen H, Lin B, Han P, Li C, Zhang Q, et al. Docking study and antiosteoporosis effects of a dibenzylbutane lignan isolated from *Litsea cubeba* targeting cathepsin K and MEK1. *Med Chem Res* 2018; **27**: 2062-2070.

[17]Pang B, Yu XT, Zhou Q, Zhao TY, Wang H, Gu CJ, et al. Effect of *Rhizoma coptidis* (Huang Lian) on treating diabetes mellitus. *Evid Based Complement Alternat Med* 2015; **2015**: 921416.

[18]Cui X, Qian DW, Jiang S, Shang EX, Zhu ZH, Duan JA. *Scutellariae radix* and *Coptidis rhizoma* improve glucose and lipid metabolism in T2DM rats *via* regulation of the metabolic profiling and MAPK/PI3K/Akt signaling pathway. *Int J Mol Sci* 2018; **19**(11): 3634.

[19]Oyedemi SO, Nwaogu G, Chukwuma CI, Adeyemi OT, Matsabisa MG, Swain SS, et al. Quercetin modulates hyperglycemia by improving the pancreatic antioxidant status and enzymes activities linked with glucose metabolism in type 2 diabetes model of rats: *In silico* studies of molecular interaction of quercetin with hexokinase and catalase. *J Food Biochem* 2019; **26**: e13127.

[20]Ebrahimpour S, Esmaeili A, Beheshti S. Effect of quercetin-conjugated superparamagnetic iron oxide nanoparticles on diabetes-induced learning and memory impairment in rats. *Int J Nanomed* 2018; **13**: 6311-6324.

[21]Shen Y, Guan S, Ge H, Xiong W, He L, Liu L, et al. Effects of palmatine on rats with comorbidity of diabetic neuropathic pain and depression. *Brain Res Bull* 2018; **139**: 56-66.

[22]Heinzel A, Kammer M, Mayer G, Reindl-Schwaighofer R, Hu K, Perco P, et al. Validation of plasma biomarker candidates for the prediction of EGFR decline in patients with type 2 diabetes. *Diabetes Care* 2018; **41**(9): 1947-1954.

[23]Akbari M, Hassan-Zadeh V. IL-6 signalling pathways and the development of type 2 diabetes. *Inflammopharmacology* 2018; **26**(3): 685-698.

[24]Maellaro E, Leoncini S, Moretti D, Del Bello B, Tanganelli I, De Felice C, et al. Erythrocyte caspase-3 activation and oxidative imbalance in erythrocytes and in plasma of type 2 diabetic patients. *Acta Diabetol* 2013; **50**(4): 489-495.

[25]Ahrén Bo. Islet G protein-coupled receptors as potential targets for treatment of type 2 diabetes. *Nat Rev Drug Discov* 2009; **8**(5): 369-385.

[26]Huang X, Liu G, Guo J, Su Z. The PI3K/AKT pathway in obesity and type 2 diabetes. *Int J Biol Sci* 2018; **14**(11): 1483-1496.

[27]Fang YW, Wang SY, Wu JH. The kinetics and mechanism of α-glucosidase inhibition by F5-SP, a novel compound derived from sericin peptides. *Food Funct* 2017; **8**(1): 323-332.

[28]Tundis R, Loizzo MR, Menichini F. Natural products as α-amylase and α-glucosidase inhibitors and their hypoglycaemic potential in the treatment of diabetes: An update. *Mini Rev Med Chem* 2010; **10**(4): 315-331.

[29]Fukami K, Yamagishi S, Ueda S, Okuda S. Role of ages in diabetic nephropathy. *Curr Pharm Design* 2008; **14**(10): 946.

[30]Matsui T, Yamagishi SI. Advanced glycation end products (AGEs), oxidative stress and diabetic retinopathy. *Curr Pharm Biotechnol* 2011; **12**(3): 362-368.

[31]Lv X, Lv GH, Dai GY, Sun HM, Xu HQ. Food-advanced glycation end products aggravate the diabetic vascular complications *via* modulating the AGEs/RAGE pathway. *Chine J Nat Med* 2016; **14**(11): 844-855.

Network pharmacology-based analysis of effective components and mechanism of Rhizoma coptidis in treating diabetes

Qianqian Zeng[1,#], Jiawei Cai[1,#], Yue Xu[1], Lin Li[2], Qiu Chen[1,*], Rensong Yue[1,*]

1. Hospital of Chengdu University of Traditional Chinese Medicine, Chengdu 610072, P.R. China;

2. School of Pharmacy, Chengdu University of Traditional Chinese Medicine, Chengdu, 611130, PR China

*Correspondence author: Qiu Chen;

Correspondence address: Hospital of Chengdu University of Traditional Chinese Medicine, No. 39 Shi-er-qiao Road, Chengdu 610072, P.R. China;

Phone and Fax: 028-87766249；

E-mail: chenqiu1005 @cdutcm.edu.cn

*Correspondence author: Rensong Yue;

Correspondence address: Hospital of Chengdu University of Traditional Chinese Medicine, No. 39 Shi-er-qiao Road, Chengdu 610072, P.R. China;

Phone and Fax: 028-87780687；

E-mail: songrenyue@cdutcm.edu.cn

# Qianqian Zeng and Jiawei Cai contributed equally to this paper.

Supplementary Table 1. The GO functions of overlapping target genes.

ID	Description	P value	P.adjust	Q value	Gene ID	Count
GO:0004879	nuclear receptor activity	0.00000009	0.00001520	0.00000969	ESR1/AR/ESR2/PPARG/AHR/NR1I3	6
GO:0098531	transcription factor activity, direct ligand regulated sequence-specific DNA binding	0.00000009	0.00001520	0.00000969	ESR1/AR/ESR2/PPARG/AHR/NR1I3	6
GO:0003707	steroid hormone receptor activity	0.00000026	0.00002960	0.00001890	ESR1/AR/NR3C2/ESR2/PPARG/NR1I3	6
GO:0008227	G protein-coupled amine receptor activity	0.00000035	0.00003040	0.00001940	CHRM3/CHRM1/CHRM5/ADRA2C/ADRA1A/CHRM2	6
GO:0001085	RNA polymerase II transcription factor binding	0.00000072	0.00004960	0.00003170	ESR1/AR/PPARG/FOS/RB1/ELK1/NFE2L2/AHR	8
GO:0001228	DNA-binding transcription activator activity, RNA polymerase II-specific	0.00000105	0.00006050	0.00003870	ESR1/AR/RELA/FOS/ELK1/HIF1A/MYC/NFE2L2/PARP1/NR1I3/RUNX2/IRF1	12
GO:0030594	neurotransmitter receptor activity	0.00000137	0.00006780	0.00004330	CHRM3/CHRM1/CHRM5/HTR3A/CHRM2/GABRA1/GRIA2	7
GO:0044389	ubiquitin-like protein ligase binding	0.00000195	0.00008430	0.00005390	RELA/EGFR/BCL2/RB1/NFKBIA/CASP8/HIF1A/CCNB1/CHEK2/ERBB3	10
GO:0033613	activating transcription factor binding	0.00000309	0.00011892	0.00007600	PPARG/RELA/FOS/RB1/MYC/NFE2L2	6
GO:0015464	acetylcholine receptor activity	0.00000390	0.00013508	0.00008630	CHRM3/CHRM1/CHRM5/CHRM2	4
GO:0005496	steroid binding	0.00000592	0.00018619	0.00011895	ESR1/AR/NR3C2/ESR2/CYP3A4/CAV1	6
GO:0031625	ubiquitin protein ligase binding	0.00000946	0.00027263	0.00017418	RELA/EGFR/BCL2/RB1/NFKBIA/CASP8/HIF1A/CHEK2/ERBB3	9
GO:0043295	glutathione binding	0.00001660	0.00044078	0.00028161	GSTP1/GSTM1/GSTM2	3
GO:0004993	G protein-coupled serotonin receptor activity	0.00001960	0.00045325	0.00028958	CHRM3/CHRM1/CHRM5/CHRM2	4

GO:0099589	serotonin receptor activity	0.00001960	0.00045325	0.00028958	CHRM3/CHRM1/CHRM5/CHRM2	4
GO:1900750	oligopeptide binding	0.00002200	0.00047587	0.00030403	GSTP1/GSTM1/GSTM2	3
GO:0016653	oxidoreductase activity, acting on NAD(P)H, heme protein as acceptor	0.00002850	0.00058025	0.00037071	POR/NOS3/NQO1	3
GO:0005178	integrin binding	0.00003880	0.00070844	0.00045261	EGFR/PRKCA/ICAM1/VCAM1/COL3A1/IGF2	6
GO:0051879	Hsp90 protein binding	0.00004180	0.00070844	0.00045261	HIF1A/CYP1A1/AHR/HSF1	4
GO:0099528	G protein-coupled neurotransmitter receptor activity	0.00004180	0.00070844	0.00045261	CHRM3/CHRM1/CHRM5/CHRM2	4

Network pharmacology-based analysis of effective components and mechanism of Rhizoma coptidis in treating diabetes

Qianqian Zeng[1,#], Jiawei Cai[1,#], Yue Xu[1], Lin Li[2], Qiu Chen[1,*], Rensong Yue[1,*]

1. Hospital of Chengdu University of Traditional Chinese Medicine, Chengdu 610072, P.R. China;

2. School of Pharmacy, Chengdu University of Traditional Chinese Medicine, Chengdu, 611130, PR China

*Correspondence author: Qiu Chen;

Correspondence address: Hospital of Chengdu University of Traditional Chinese Medicine, No. 39 Shi-er-qiao Road, Chengdu 610072, P.R. China;

Phone and Fax: 028-87766249；

E-mail: chenqiu1005 @cdutcm.edu.cn

*Correspondence author: Rensong Yue;

Correspondence address: Hospital of Chengdu University of Traditional Chinese Medicine, No. 39 Shi-er-qiao Road, Chengdu 610072, P.R. China;

Phone and Fax: 028-87780687；

E-mail: songrenyue@cdutcm.edu.cn

# Qianqian Zeng and Jiawei Cai contributed equally to this paper.

Supplementary Table 2. The KEGG pathways of overlapping target genes.

ID	Description	P value	P.adjust	Q value	Gene ID	Count
hsa05418	Fluid shear stress and atherosclerosis	0.0000000001	0.0000000134	0.0000000063	RELA/VEGFA/BCL2/FOS/CAV1/ICAM1/SELE/VCAM1/NOS3/GSTP1/NFE2L2/NQO1/GSTM1/GSTM2	14
hsa05215	Prostate cancer	0.0000000001	0.0000000149	0.0000000071	AR/RELA/EGFR/CCND1/BCL2/CASP9/PLAU/RB1/NFKBIA/RAF1/ERBB2/GSTP1	12
hsa04933	AGE-RAGE signaling pathway in diabetic complications	0.0000000002	0.0000000149	0.0000000071	RELA/VEGFA/CCND1/BCL2/IL6/CASP3/PRKCA/ICAM1/SELE/VCAM1/NOS3/COL3A1	12
hsa05161	Hepatitis B	0.0000000005	0.0000000263	0.0000000124	RELA/BCL2/FOS/CASP9/RB1/IL6/CASP3/ELK1/NFKBIA/CASP8/RAF1/PRKCA/MYC/BIRC5	14
hsa05205	Proteoglycans in cancer	0.0000000011	0.0000000459	0.0000000217	ESR1/EGFR/VEGFA/CCND1/PLAU/CASP3/ELK1/RAF1/PRKCA/HIF1A/ERBB2/CAV1/MYC/IGF2/ERBB3	15
hsa05167	Kaposi sarcoma-associated herpesvirus infection	0.0000000030	0.0000001086	0.0000000514	RELA/VEGFA/CCND1/FOS/CASP9/RB1/IL6/CASP3/NFKBIA/CASP8/RAF1/HIF1A/MYC/ICAM1	14
hsa05163	Human cytomegalovirus infection	0.0000000041	0.0000001274	0.0000000603	RELA/EGFR/VEGFA/CCND1/CASP9/RB1/IL6/CASP3/ELK1/NFKBIA/CASP8/RAF1/PRKCA/MYC/PTGER3	15
hsa05219	Bladder cancer	0.0000000049	0.0000001329	0.0000000629	EGFR/VEGFA/CCND1/RB1/RAF1/ERBB2/MYC/RASSF1	8
hsa05225	Hepatocellular carcinoma	0.0000000083	0.0000002019	0.0000000955	EGFR/CCND1/RB1/ELK1/RAF1/PRKCA/MYC/GSTP1/NFE2L2/NQO1/IGF2/GSTM1/GSTM2	13
hsa04115	p53 signaling pathway	0.0000000306	0.0000006669	0.0000003156	CCND1/BCL2/CASP9/CASP3/CASP8/CCNB1/CHEK2/IGFBP3/CHEK1	9
hsa01524	Platinum drug resistance	0.0000000346	0.0000006860	0.0000003246	BCL2/CASP9/CASP3/CASP8/ERBB2/BIRC5/GSTP1/GSTM1/GSTM2	9
hsa04210	Apoptosis	0.0000000825	0.0000014983	0.0000007090	RELA/BCL2/FOS/CASP9/CASP3/NFKBIA/CASP8/RAF1/BIRC5/PARP1/CTSD	11

hsa04066	HIF-1 signaling pathway	0.0000001016	0.0000017046	0.0000008066	RELA/EGFR/VEGFA/BCL2/IL6/PRKCA/HIF1A/ERBB2/NOS3/HK2	10
hsa04668	TNF signaling pathway	0.0000001317	0.0000020514	0.0000009707	RELA/FOS/IL6/CASP3/NFKBIA/CASP8/ICAM1/SELE/VCAM1/IRF1	10
hsa05210	Colorectal cancer	0.0000001478	0.0000021481	0.0000010165	EGFR/CCND1/BCL2/FOS/CASP9/CASP3/RAF1/MYC/BIRC5	9
hsa05223	Non-small cell lung cancer	0.0000002401	0.0000032712	0.0000015480	EGFR/CCND1/CASP9/RB1/RAF1/PRKCA/ERBB2/RASSF1	8
hsa04151	PI3K-Akt signaling pathway	0.0000002844	0.0000036464	0.0000017255	CHRM1/CHRM2/RELA/EGFR/VEGFA/CCND1/BCL2/CASP9/IL6/RAF1/PRKCA/ERBB2/MYC/NOS3/IGF2/ERBB3	16
hsa01522	Endocrine resistance	0.0000004596	0.0000055658	0.0000026337	ESR1/ESR2/EGFR/CCND1/BCL2/FOS/RB1/RAF1/ERBB2	9
hsa05212	Pancreatic cancer	0.0000007277	0.0000083495	0.0000039510	RELA/EGFR/VEGFA/CCND1/CASP9/RB1/RAF1/ERBB2	8
hsa04010	MAPK signaling pathway	0.0000009809	0.0000102046	0.0000048288	RELA/EGFR/VEGFA/FOS/CASP3/ELK1/RAF1/PRKCA/ERBB2/MYC/HSPB1/IGF2/ERBB3/RASA1	14